Stochastic resonance in a biological motor under complex fluctuations

Cheng-Hung Chang[1] and Tian Yow Tsong[2,3]
[1]*National Center for Theoretical Sciences, Physics Division, Hsinchu 300, Taiwan*
[2]*University of Minnesota, College of Biological Science, St. Paul, Minnesota 55108, USA*
[3]*Department of Physics, National Taiwan University, Taipei, Taiwan*
(Received 21 March 2003; revised manuscript received 12 May 2003; published 27 February 2004)

The dynamics division approach proposed in this work enables us to handle dynamical equations with complex fluctuations. A Brownian motor with cyclic conformational changes is analyzed to understand effects of noise on its signal transduction, and on condition in which stochastic resonance may take place. The result reproduces several features of the experimental data on the electric activation of ion pumping by Na, K-ATPase.

DOI: 10.1103/PhysRevE.69.021914 PACS number(s): 82.39.Fk, 82.39.−k, 87.15.Aa

The fabrication of nanometer scale devices has made significant stride recently by clever modeling after the biological motors. Examples include the artificial photosynthetic membrane using light to transport calcium ions [1], the microscopic propeller attached to an ATPase to drive particle motion [2], and the artificial nanometer pores when stimulated by electric field transport potassium ions against concentration gradient [3]. The interest in this area accents the importance of a precise understanding on the fundamental principles and mechanisms that operate on the biological motors. These motors are ubiquitous in the living systems, for example, the DNA packaging motor, bacteriophage $\phi 29$ [4], the vesicle transporter, kinesin [5], the energy transducer F_1 ATPase [6], and the ion pump Na, K-ATPase [5].

An essential attribute of these motors is that the energy transduction and material transport are accomplished by the cyclic conformational changes of the enzymes [7,9](l). This cyclic motion can be described by a Langevin equation, which in general is nonlinear for a driving force term. Since the fluctuation is considerably large for a nanoscale motor of small inertia [8], the fluctuation dominates the force term. An erratic fluctuation in the nonlinear term, however, poses a difficulty in deriving the Fokker-Planck equation. Therefore, analytical solution on the probability evolution is hard to obtain. This difficulty cannot be circumvented even by the conventional numerical analysis because these methods are based on the smoothness of noiseless differential equations. Consequently, the previous study has been limited to the behavior of simple enzyme models under primitive fluctuations, e.g., the 2- and 4-state models of the ion pump [9] in Fig. 1 under the monochromatic fluctuations in Table I. More complex systems have rarely been analyzed besides the recent theoretical work of Fulinski and co-workers [10]. However, their studies are based on Shapiro's theory, which is applicable only to the dichotomous noise. The fluctuation encountered in a living cell is likely to be much more complex, and a deeper understanding of the role of polychromatic noises is warranted.

The approach presented in this work attempt to overcome this difficulty. We divide the dynamics of the Langevin equation into a number of subdynamics of shorter time intervals, with constant fluctuation values. The final state of a subdynamics is the initial state of the next subdynamics. The noise is given by reducing the time intervals of the subdynamics. With the Brownian ion pump shown in Fig. 1, the main features computed with this approach agree with that of the analytical approach using the concept of the intrinsic noise [10], as well as the experimental observations of the Na, K-ATPase [9](k). These agreements point to the merit of the present approach. Furthermore, our results extend beyond the previous studies and reveal conditions in which stochastic resonance may take place. These latter results may be subject to future experimental test.

Na, K-ATPase is a molecular motor, whose mechanism of action is shown to be consistent with the flashing ratchet [9,11]. The enzyme is a transmembrane protein complex, which can pump Na^+, K^+ ions against the concentration gradients across the cell membrane. In a cell the energy required for the active transport is derived from the hydrolysis of ATP (adenosine triphosphate) or from the fluctuation of the transmembrane electric potential [9](d), [10]. This latter effect provides a convenient system for the theoretical analysis and is of fundamental interest for the future devices in

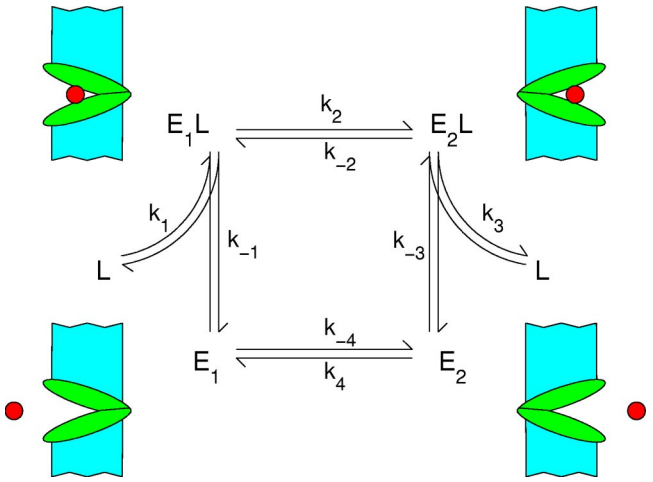

FIG. 1. The 4-state kinetic model of a transmembrane enzyme motor. The enzyme is depicted by the pacmans with two different opening orientations. The ligand is depicted by the ball. A 2-state model is the extreme case when k_2 and k_4 are much larger or smaller than k_{-2} and k_{-4}, such that the kinetic model can be simplified to only two states EL and E.

TABLE I. Fluctuations used to study Na, K, ion pump, with the abbreviations: RTF (random-telegraph fluctuation), DS (stochastic dichotomous signal), DN (intrinsic dichotomous noise), and WN (white noise).

References	Model	Fluctuations	Expt. or Theor.
[9](a)	4-state	cos	Expt.+Theor.
[9](c)	4-state	RTF	Expt.+Theor.
[9](d)	2-state	cos	Theor.
[9](e)	4-state	cos	Expt.+Theor.
[9](f)	4-state	cos	Theor.
[9](g)	4-state	Square	Theor.
[9](h)	2-state	Square	Theor.
[9](i)		cos, square, RTF	Expt.
[10]	2-state	cos, DS+DN	Theor.
[9](j)	4-state	RTF	Theor.+Expt.
[9](k)	4-state	RTF, cos+WN	Expt.

nanobiotechnology, such as the recent artificial ion pump driven by external field [3]. Fulinski and co-workers [10] have introduced an intrinsic electric noise, presumably generated by the concentration fluctuation of ions near the ion channel (see also Ref. [9](b)). This noise is then coupled to the externally applied electric signal to drive ion pumping. In the experiment of Tsong and Xie [9](k), an externally applied electric noise is superimposed on an electric signal to drive ion transport. Both studies observe stochastic resonance phenomena [12].

In these studies theory of electroconformational coupling (TEC) has been cited. The TEC model states that each enzyme conformation has an electric moment associated with it and a conformational change will produce a change in the molar electric moment [9](a). A proper field oscillation will thus drive an enzyme conformational oscillation. This will allow the enzyme to harvest energy from the applied field [9]. Figure 1 depicts a kinetic model of a transporter. Here the transporter can assume four conformations with certain kinetic rate constants k_i's that define the probabilities of the enzyme in different conformations. Suppose the rate constants k_i's are time independent and the enzyme, which opens to the left (right) hand side of the membrane, prefers to bind the ligand (release the ligand) under certain $k_{\pm 1}$ and $k_{\pm 3}$. Then the enzyme concentrations in Fig. 1 tend to flow from E_1 (E_2L) to E_1L (E_2) and finally converge to an equilibrium state, with more concentration distributed on E_1L and E_2. However, the equilibrium can be broken, when a force is applied to change the rate constants and activate the processes from E_1L (E_2) to E_2L (E_1), which shifts the ligand across the membrane. After the enzyme releases the ligand (binds a new ligand) on the right (left) hand side, the force is lifted, which drives the enzyme conformations back to the original equilibrium state again. A proper force oscillation then generates a clockwise flow, which transports the ligand from left to right.

The kinetic equation for the concentrations of the four conformations in Fig. 1 is a four-dimensional nonautonomous linear dynamical system

$$\frac{d}{dt}V(t)=M(t)V(t), \tag{1}$$

with the concentration state

$$V(t)=\begin{pmatrix}[E_2L]\\ [E_1L]\\ [E_2]\\ [E_1]\end{pmatrix}$$

and the time dependent

$$M(t)=\begin{pmatrix}-k_3-k_{-2} & k_2 & k_{-3}[L_3] & 0\\ k_{-2} & -k_{-1}-k_2 & 0 & k_1[L_1]\\ k_3 & 0 & -k_4-k_{-3}[L_3] & k_{-4}\\ 0 & k_{-1} & k_4 & -k_{-4}-k_1[L_1]\end{pmatrix},$$

where the sum of the four conformation concentrations in $V(t)$ is conserved. The values $[L_1]$ and $[L_3]$ in $M(t)$ denote the concentrations of L on the left and right hand side of the membrane, respectively, which can be regarded as constants, if the time observed is not too long. The rate constants $k_i=h_i\exp[q_i\phi(t)a_i/RT]$ for $i\in\{\pm 1,\pm 2,\pm 3,\pm 4\}$, consist of the gas constant R, the temperature T, the effective charge q_i of different enzyme conformations, the transmembrane potential $\phi(t)$, the rate constant h_i in zero potential $\phi(t)=0$, and the apportionment constant a_i, which splits up the total energy $q_i\phi(t)$ into two parts, corresponding to forward and backward chemical processes, and obeys the relation $a_j=\delta_j$ and $a_{-j}=-(1-\delta_j)$ for certain δ_j with $j\in\{1,2,3,4\}$ [9]. The values k_i's are positive, time dependent, and can be simplified to the form $k_i=h_i\exp[d_i\psi(t)]$, characterized by parameters h_i, d_i and the fluctuation $\psi(t)$. The instantaneous flux of the transported ligands can be determined by $j(t)=k_3[E_2L]-k_{-3}[E_2][L_3]$, which yields the transported amount $S(t)=\int_0^t j(t')\,dt'$. The motor can perform transport when the averaged flux J is nonzero, where $J=\lim_{t\to\infty}S(t)/t$ or $J=S(\tau)/\tau$, if $S(t)$ is periodic with period τ.

Figure 2(a) shows the concentration evolutions and the

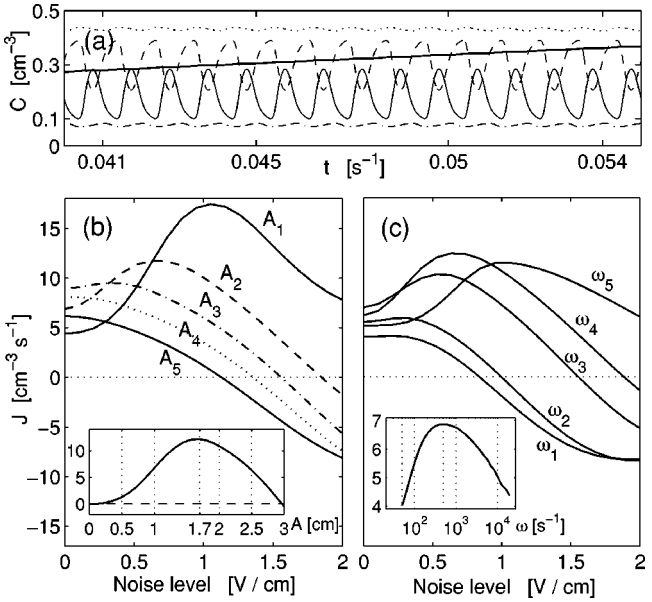

FIG. 2. (a) The oscillations of different concentrations $[E_1]$ (dotted), $[E_2]$ (dash-dotted), $[E_1L]$ (thin solid), $[E_2L]$ (dashed), induced by $\psi(t)=\sin(\omega t)$, and the positive transported amount $S(t)$ across the membrane (thick solid). (b) The averaged flux J vs the noise level η under five different amplitudes of sinusoidal signal with signal frequency $\omega=10^3$ and $\omega_n/\omega=10^3$, where $A_1=0.5$, $A_2=1$, $A_3=1.4$, $A_4=1.7$, and $A_5=2$. The inset shows the signal amplitude dependence of the averaged flux J without noise. (c) The averaged flux J vs the noise level η under five different signal frequencies ω's with signal amplitude $A=1$ and $\omega_n/\omega=10^3$, where $\omega_1=50$, $\omega_2=10^2$, $\omega_3=500$, $\omega_4=10^3$, and $\omega_5=10^4$. The inset shows the frequency dependence of the averaged flux J without noise.

net transported amount $S(t)$ under parameter values:

i	1	−1	2	−2	3	−3	4	−4
d_i (cm/V)	0	0	−2	−3	0	0	4	−2
h_i (s^{-1})	40*	60	25700	12000	70	200*	20	10

and $[L_1]=[L_2]=1$ cm^{-3} (h_1 and h_{-3} have dimension cm^3/s). The values $d_{\pm1}$ and $d_{\pm3}$ are set to zero, because the ligand association with and dissociation from the enzyme are less affected by the fluctuation $\psi(t)$. Notably, a nonzero J is nontrivial only when the clockwise and the counterclockwise reactions in Fig. 1 are of equal probability, which is generic in real enzymes and guaranteed by the detailed balance condition $\Pi_{i=1}^4 h_i=\Pi_{i=1}^4 h_{-i}$.

The dynamical system (1) is dissipative at any instantaneous time t, due to the negative gradient $\nabla[M(t)V(t)]=\Sigma_{i=1}^4 M_{ii}(t)<0$. In the absence of the applied field $\psi(t)$, the values k_i's and the matrix $M(t)$ are constant in time. Any state $V(t)$ converges to the stable fixed point V_0 of Eq. (1) with the property $[E_2][L_3]/[E_2L]=k_3/k_{-3}$, which leads to the vanishing $j(t)$, $S(t)$, and J. In the presence of $\psi(t)$, the matrix $M(t)$ is time dependent. A state in Eq. (1) tends to converge to the instantaneous fixed point $V_0(t)$, however, it does not stick to any point, because the vector field of Eq. (1) never becomes stationary and $V_0(t)$ is moving in time. The

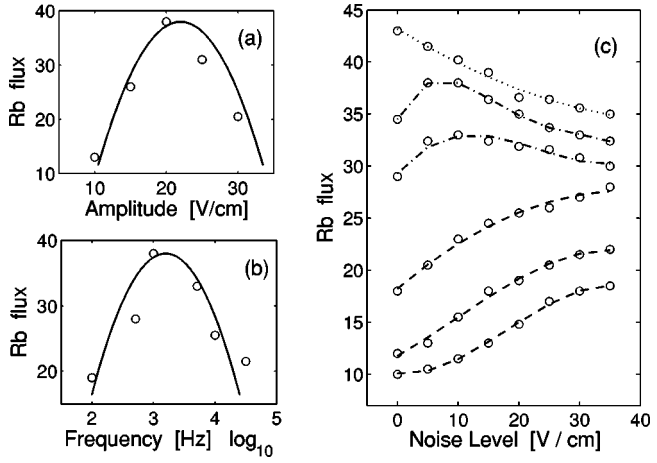

FIG. 3. Electric field induced rubidium pumping of Na, K-ATPase in Ref. [12]: flux [amole/hour] vs (a) amplitude of the RTF with mean frequency 1 kHz; (b) amplitude of the RTF with amplitude 20 V/cm; (c) noise level η under sinusoidal signal with amplitude 20 V/cm and frequency 1 kHz. The curves have signal amplitudes 20, 17.5, 15, 12.5, 10, and 7.5 V/cm from top to bottom.

study on various models [9] indicates that an exactly zero J is uncommon and a transport always occurs when the fluctuation is appropriately selected, which is expected since the k_i values in the cyclic wheel in Fig. 1 are asymmetric in general. Therefore, the more important issue in the study of micromotors should not be whether a motor works, but how does it precisely work under diverse complex fluctuation sources.

The fluctuation $\psi(t)$ in a real system usually consist of different sources, such as a signal combined with the intrinsic noise activated by the ion channels [10,13]. The following study focuses on the concrete example $\psi(t)=A\sin(\omega t)+\xi(t)$, with a dominating signal $A\sin(\omega t)$ and a secondary noise $\xi(t)$, where A denotes the signal amplitude. The dynamics division approach described in the second paragraph is applied to $\psi(t)$ with the step noise, however, only under two periodically repeating values $\xi\in\{\pm1\}$ of frequency ω_n, for the purpose of obtaining a stationary J under limited time and computation resource. The noise strength is in the scale of noise level $\eta=\eta_{rms}/A$ with the root mean square $\eta_{rms}=\sqrt{\int_0^\tau \xi(t)^2\,dt/\tau}$, where $\tau=1/\omega_n$ denotes the period of the noise. The simulated results are performed under the ratio $\omega_n/\omega=10^3$ and its stability is confirmed by the convergent results under increasing ω_n/ω from 10^3 to 10^4.

The inset in Fig. 2(b) shows the amplitude dependence of the averaged flux J without noise. The optimal signal amplitude A_{op} for the transport is around $A=1.7$. If the signal amplitude is too large, e.g., $A>3$, the value J can be negative and current reversal can occur. This is similar to the current reversal phenomena in various ratchet models [14]. Taking five different amplitudes from the inset, the curves of the flux J versus η in Fig. 2(b) indicate the destructive influence of the noise on the transport in large noise regime, such as $\eta>1.5$, which even induces current reversal. This destructive role of the noise is intuitive from our experience on the motors in the macroworld. However, this is not always true

for small noise, e.g., $\eta < 0.5$, in which the noise is constructive for $A < A_{op}$ and destructive for $A \geqslant A_{op}$. Since the curve for $A = 0.5$ is still quite flat at $\eta = 2$, it is unclear whether all amplitudes have current reversal, when the noise strength is infinitely large.

The inset in Fig. 2(c) shows the frequency dependence of the averaged flux J without noise. The apparent peak indicates the natural frequency $\omega_{op} = 500$, which is the optimal frequency of the system. Taking five frequencies from the inset, the flux J decreases monotonically, for small frequency such as $\omega = 50$. Other larger frequencies exhibit a bell shape and imply the stochastic resonance, which can be recognized after replotting the figure to a ratio of J/η_{rms} versus η_{rms}, as that in Ref. [10]. Similar to the plot in Fig. 2(b), the transport efficiencies in Fig. 2(c) decrease for strong noise. However, different from the plot in Fig. 2(b), the noise in Fig. 2(c) is constructive for both $\omega < \omega_{op}$ and $\omega \geqslant \omega_{op}$ in the weak noise regime, up to the slow signal such as $\omega = 50$.

Similar features as in Figs. 2(b) and 2(c) can be found in Fig. 3, which are measured in the experiment of the rubidium transport across the human red cell membrane [9](k). The plot from random-telegraph fluctuation (RTF) in Figs. 3(a) and 3(b) have similar bell shapes as those in the insets of Figs. 2(b) and 2(c) under sinusoidal fluctuation. The dotted, dashed, and dash-dotted curve families in Fig. 3(c) have decreasing, increasing, and bell-shaped features, which are the same as the features of the dotted, dashed, and dash-dotted curves in Fig. 2(b) in the small noise strength regime, e.g., $\eta < 0.6$. However, the decreasing transport efficiency after A_{op} predicted in Fig. 2(b) as well as the curves in the main plot of Fig. 2(c) are beyond the experimental data and need further investigation.

Both the experimental observations and the numerical results calculated by the dynamics division approach lead to similar conclusions that the noise is destructive, when the amplitude of the signal A is optimal for transport. However, a noise of proper amplitude may improve transport efficiency and produce stochastic resonance when the signal is suboptimal. This phenomenon seems to be the same for different kinds of noise. This latter observation is not surprising for when a noise is weak, it can be regarded as a secondary perturbation term to the dynamical system, Eq. (1). A slight change in a perturbation term is much less likely to produce a dramatic change on system dynamics. Finally, we would like to point out that the result of this study augments that of Fulinski *et al.* Ion concentration fluctuation in the vicinity of an enzyme can cause fluctuation in transmembrane electric potential, which in turn, may generate conformational fluctuation of the transporter.

This work was supported by the National Science Council in Taiwan, under Contract No. NSC 90-2112-M-007-067.

[1] I.M. Bennett *et al.*, Nature (London) **420**, 398 (2002).

[2] C. Montemagno and G. Bachand, Nanotechnology **10**, 225 (1999); R.K. Soong *et al.*, Science **290**, 1555 (2000).

[3] Z. Siwy and A. Fuliński, Phys. Rev. Lett. **89**, 198103 (2002); J.R. Minkel, Phys. Rev. Focus **10**, 19 (2002).

[4] National Science Foundation News, 2000, http://www.nsf.gov/od/lpa/news/press/00/pr0092.htm

[5] See, for instance, H. Lodish *et al.*, *Molecular Cell Biology* (Freeman, New York, 2000).

[6] H. Noji, R. Yasuda, M. Yoshida, and K.J. Kinosita, Nature (London) **386**, 299 (1997).

[7] Press release: The 1997 Nobel prize in chemistry, http://www.nobel.se/chemistry/laureates/1997/press.html

[8] R.D. Astumian and P. Hänggi, Phys. Today **55**(11), 33 (2002); E. Purcell, Am. J. Phys. **45**, 3 (1977).

[9] (a) T.Y. Tsong and R.D. Astumian, Bioelectrochem. Bioenerg. **15**, 457 (1986); (b) Prog. Biophys. Mol. Biol. **50**, 1 (1987); (c) R.D. Astumian, P.B. Chock, T.Y. Tsong, Y.-D. Chen, and H.V. Westerhoff, Proc. Natl. Acad. Sci. U.S.A. **84**, 434 (1987); (d) R.D. Astumian, P.B. Chock, T.Y. Tsong, and H.V. Westerhoff, Phys. Rev. A **39**, 6416 (1989); (e) D.S. Liu, R.D. Astumian, and T.Y. Tsong, J. Biol. Chem. **265**, 7260 (1990); (f) B. Robertson and R.D. Astumian, Biophys. J. **57**, 689 (1990); **58**, 969 (1990); J. Chem. Phys. **94**, 7414 (1991); (g) V.S. Markin and T.Y. Tsong, Biophys. J. **59**, 1308 (1991); (h) Y.-D. Chen and T.Y. Tsong, *ibid.* **66**, 2151 (1994); (i) T.D. Xie, P. Marszalek, Y.-D. Chen, and T.Y. Tsong, *ibid.* **67**, 1247 (1994); (j) T.D. Xie, Y.-D. Chen, P. Marszalek, and T.Y. Tsong, *ibid.* **72**, 2496 (1997); (k) T.Y. Tsong and T.D. Xie, Appl. Phys. A: Mater. Sci. Process. **75**, 345 (2002); (l) T.Y. Tsong and C.-H. Chang, AAPPS Bulletin **13**, 12 (2003).

[10] A. Fuliński, Phys. Rev. Lett. **79**, 4926 (1997); Chaos **8**, 549 (1998); A. Fuliński and P.F. Góra, Phys. Rev. E **64**, 011905 (2001).

[11] P. Reimann, Phys. Rep. **361**, 57 (2002); R.D. Astumian, Science **276**, 917 (1997); F. Jüdlicher, A. Ajdari, and J. Prost, Rev. Mod. Phys. **69**, 1269 (1997); R.D. Astumian, Eur. Biophys. J. **27**, 474 (1998).

[12] L. Gammaitoni, P. Hänggi, P. Jung, and F. Marchesoni, Rev. Mod. Phys. **70**, 223 (1998); K. Wiesenfeld and F. Moss, Nature (London) **373**, 33 (1995).

[13] H. Salman, Y. Soen, and E. Braun, Phys. Rev. Lett. **77**, 4458 (1996).

[14] J.L. Mateos, Phys. Rev. Lett. **84**, 258 (2000); P. Jung, J.G. Kissner, and P. Hänggi, *ibid.* **76**, 3436 (1996).